Inorganic Chemistry
Article
pubs.acs.org/IC

Synthesis, Crystal Structure and Catalytic Behavior of Homo- and Heteronuclear Coordination Polymers [M(tdc)(bpy)] (M^{2+} = Fe^{2+}, Co^{2+}, Zn^{2+}, Cd^{2+}; tdc^{2-} = 2,5-thiophenedicarboxylate)

Florian Kettner,[†] Christian Worch,[†] Jens Moellmer,[‡] Roger Gläser,[†] Reiner Staudt,[§] and Harald Krautscheid*[,†]

[†]Universität Leipzig, Fakultät für Chemie und Mineralogie, Johannisallee 29, 04103 Leipzig, Germany
[‡]Institut für Nichtklassische Chemie e.V., Permoserstrasse 15, 04318 Leipzig, Germany
[§]Fachhochschule Offenburg, Fakultät für Maschinenbau und Verfahrenstechnik, Badstrasse 24, 77652 Offenburg, Germany

Supporting Information

ABSTRACT: A series of isostructural 3D coordination polymers $^3_\infty$[M(tdc)(bpy)] (M^{2+} = Zn^{2+}, Cd^{2+}, Co^{2+}, Fe^{2+}; tdc^{2-} = 2,5-thiophenedicarboxylate; bpy = 4,4′-bipyridine) was synthesized and characterized by X-ray diffraction, thermal analysis, and gas adsorption measurements. The materials show high thermal stability up to approximately 400 °C and a solvent induced phase transition. Single crystal X-ray structure determination was successfully performed for all compounds after the phase transition. In the zinc-based coordination polymer, various amounts of a second type of metal ions such as Co^{2+} or Fe^{2+} could be incorporated. Furthermore, the catalytic behavior of the homo- and heteronuclear 3D coordination polymers in an oxidation model reaction was investigated.

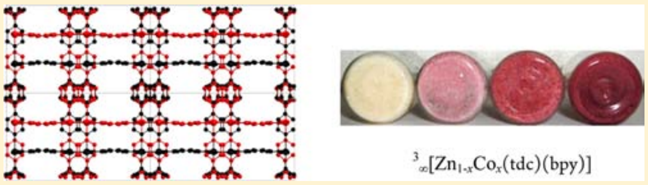

INTRODUCTION

During the past decade, interest in metal–organic frameworks (MOFs) has increased significantly due to various potential applications of these materials, e.g. gas adsorption, gas separation, catalysis, or energy storage.[1–4] Many compounds with promising properties such as HKUST-1[5] or DUT-6[6] were synthesized, but until now the breakthrough to an industrial application has not been made. For this reason, the synthesis of new MOF materials with improved properties is necessary. Often anionic and neutral ligands have been combined in order to gain three-dimensional connectivity without solvent coordination and to avoid the formation of charged frameworks. Examples are the combinations of di- or tricarboxylates with triazolyl derivatives, 4,4′-bipyridine or 1,4-diazabicyclo[2.2.2]octane (dabco).[7]

Regarding the catalytic activity of a coordination polymer, the type and properties of incorporated metal ions are important. Consequently, the approach of heteronuclear, i.e., mixed metal coordination polymers might be advantageous. In this kind of materials, various types of metal ions can assume different tasks—one type of metal ion can act as a node to form the network and another one can be responsible for the catalytic activity. In order to realize the formation of heteronuclear coordination polymers, three pathways are possible:

1. Partial, but statistical replacement of one metal species by another: This method of "isomorphous substitution" is most likely to be successful in the case of a series of isostructural compounds.[8]
2. Specific coordination of two distinct metal types by two different donor groups of the linker, following the HSAB concept[9,10] or exploiting the oxophilicity of lanthanide ions.[11,12]
3. Using metal containing linkers with additional donor groups. These have one metal species already bound in the ligand and coordinate to a second type of metal ions.[13]

Only a limited number of studies applying these methods are known and led to the formation of several heteronuclear coordination polymers. Most of these materials have promising properties, e.g., in gas adsorption, magnetism, luminescence, or catalysis.[8,12,13]

Herein we report on synthesis and properties of a series of isostructural coordination polymers $^3_\infty$[M(tdc)(bpy)] containing divalent metal ions (M^{2+} = Zn^{2+}, Cd^{2+}, Co^{2+}, Fe^{2+}) and bridging anionic 2,5-thiophenedicarboxylate (tdc^{2-}) as well as neutral 4,4′-bipyridine (bpy) linkers. In comparison with the frequently employed linear 1,4-benzenedicarboxylate ligand, the slightly bent tdc^{2-} linker is less common in coordination polymers.[14] On the basis of the isostructural character of the title compounds, we succeeded in synthesizing the mixed metal MOFs $^3_\infty$[$Zn_{1-x}Co_x$(tdc)(bpy)] and $^3_\infty$[$Zn_{1-x}Fe_x$(tdc)(bpy)]. Incorporation of Co^{2+} ions generates catalytic activity which is shown for the catalytic oxidation of cyclooctene with *tert*-butyl hydroperoxide.

Received: April 14, 2013
Published: July 18, 2013

EXPERIMENTAL SECTION

General Procedure. All syntheses were performed in stainless steel autoclaves under autogenic pressure. All chemicals were analytical reagent grade and were used as received. 2,5-Thiophenedicarboxylic acid, H_2tdc, was synthesized by a combination of the methods of Feringa et al.[15] and van Pham et al.[16]

Data sets for single crystal X-ray structure analysis were measured on IPDS-I or IPDS-2T diffractometers (STOE) and the powder diffraction patterns on a STADI-P diffractometer (STOE). The crystal structures were solved by SHELXS-97[17] and refined by SHELXL-97[17] implemented in the user interface WinGX.[18] The crystal structures are visualized using DIAMOND 3.2.[19] CHN elemental analyses were determined by a Vario EL (Elementaranalysesysteme GmbH). The metal ion content was analyzed by atomic absorption spectrometry (AAS) on an Atomic Absorption Spectrometer 3300 (Perkin-Elmer). Simultaneous thermal analyses (STA) were performed in helium atmosphere on a STA Jupiter F1 (Netzsch) coupled to a quadrupole mass spectrometer Aeolus QMS 403 C. Gas adsorption measurements were carried out on a suspension balance (Rubotherm) and on a volumetric sorption analyzer BelSorpmax (BEL Japan Inc.) according to procedures presented recently.[20,21] The gas chromatography analysis (GC-FID) of the filtrate in the catalytic test reaction was performed by a GC-2010 (Shimadzu) equipped with a RTX-5 column (Restek) of 30 m length.

Syntheses of $^3_\infty$[M(tdc)(bpy)]. 0.1 mmol $M(OAc)_2 \cdot xH_2O$ (M = Fe^{2+}, Co^{2+}, Zn^{2+}, Cd^{2+}), 0.1 mmol (17 mg) 2,5-thiophenedicarboxylic acid (H_2tdc) and 0.1 mmol (19 mg) 4,4′-bipyridine (bpy) were dissolved in 10 mL of an 1:1 mixture of methanol/water. Similar to the method described by Jia et al.[22] for the preparation of $^3_\infty$[Fe(tdc)(bpy)] and $^3_\infty$[Co(tdc)(bpy)], this mixture was heated in a Teflon lined autoclave to 120 °C, kept thermally constant for 10 h and then cooled down to room temperature within 50 h. Mixed metal derivatives were prepared by using mixtures of the metal acetates in the appropriate ratio.

Single crystals suitable for X-ray diffraction were isolated from a methanol/water mixture for the Fe, Co, and Zn compounds; the preparation of the Cd product with better crystal quality was achieved in a mixture of ethanol and water under the same conditions. In order to remove the solvent incorporated in the crystals, the products were heated up to 200 °C in air in 5 h and cooled down to room temperature in 10 h.

Yield: 65−85% (evacuated samples) of white (Zn^{2+}, Cd^{2+}), pink-violet (Co^{2+}), or brown (Fe^{2+}) crystalline product. Elemental analysis $^3_\infty$[Zn(tdc)(bpy)]: C 48.8 H 2.7 N 7.0 S 8.2% calc. for $C_{16}H_{10}N_2O_4SZn$ C 49.1 H 2.6 N 7.2 S 8.3%; $^3_\infty$[$Zn_{0.9}Co_{0.1}$(tdc)(bpy)]: C 48.8 H 2.7 N 7.1 S 8.3 Co 1.7%, calc. for $C_{16}H_{10}N_2O_4SCo_{0.1}Zn_{0.9}$ C 49.1 H 2.6 N 7.2 S 8.2 Co 1.4%; $^3_\infty$[$Zn_{0.9}Fe_{0.1}$(tdc)(bpy)]: C 48.4 H 2.8 N 6.8 S 8.3 Fe 1.3%, calc. for $C_{16}H_{10}N_2O_4SFe_{0.1}Zn_{0.9}$ C 49.2 H 2.6 N 7.2 S 8.2 Fe 1.5%. According to AAS metal analyses, the metal ratio in the heteronuclear products is close to the metal ratio applied in the synthesis (Table SI-1 of the Supporting Information, SI).

Catalytic Studies. The partial oxidation of *cis*-cyclooctene (Sigma-Aldrich) was carried out batchwise in a 50 mL round-bottom flask with magnetic stirrer and condenser. *Tert*-butyl hydroperoxide (TBHP) (Sigma-Aldrich; 5.5 M solution in *n*-decane) was used as oxidant. In a volume of 15 mL toluene (Solvadis), a molar ratio of toluene:*cis*-cyclooctene:TBHP of 70:1:3 was applied. The catalytic test reaction was performed at 75 °C for 24 h. The coordination polymer was added after the reaction mixture reached the thermal equilibrium. For each catalytic experiment, 25 mg of the catalyst (activated at 200 °C, vacuum, 16 h; Basolite C300 ([$Cu_3(btc)_2$], btc^{3-} = 1,3,5-benzenetricarboxylate; Sigma-Aldrich) activated at 120 °C, vacuum, 16 h) were added. Samples of the reaction mixture (0.3 mL) were periodically taken, separated from the catalyst, dissolved in toluene and analyzed via GC-FID.

RESULTS AND DISCUSSION

A series of isostructural coordination polymers $^3_\infty$[M(tdc)(bpy)] (M^{2+} = Zn^{2+}, Cd^{2+}, Co^{2+}, Fe^{2+}) was synthesized by reacting the metal acetates with the ligands H_2tdc and bpy. The crystal structure analyses directly after synthesis/crystallization were hampered by twinning of the crystals. In the case of as synthesized $^3_\infty$[Cd(tdc)(bpy)] the crystal structure could be solved and refined, but only with limited quality.

By careful heating of the coordination polymers a phase transition is observed in the temperature dependent X-ray powder diffraction pattern at 150 °C for the Zn^{2+}, at 110 °C for the Co^{2+} and at 90 °C for the Cd^{2+} compound (Figure 1, Figures SI1−SI3 of the SI). This phase transition is induced by the evaporation of solvent molecules localized in the pores, as demonstrated by TG-DTA experiments (coupled to MS, Figure SI4 of the SI); it was not reported before.[22] The crystal structure of as synthesized $^3_\infty$[Cd(tdc)(bpy)] can be refined in space group *P*2/*c* assuming pseudomerohedral twinning—however, only with poor quality. The symmetry changes to space group *Cmce* in the solvent free crystals (Table 1). After that transformation routine X-ray structure analysis was possible for all three compounds.

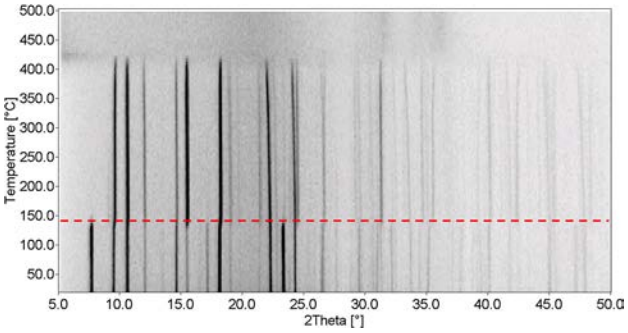

Figure 1. Temperature dependent X-ray powder diffraction pattern of as synthesized $^3_\infty$[Zn(tdc)(bpy)] from room temperature to 500 °C; Cu−$K_{\alpha 1}$ radiation (λ = 154.0598 pm).

The high temperature phases (Figure 1 and Figures SI1−SI3 of the SI) are stable after cooling down again to room temperature. These phases represent the crystal structures determined by X-ray crystallography (see Table 1).

Furthermore, all compounds $^3_\infty$[M(tdc)(bpy)] show a high thermal stability up to 400 °C which is attributed to the interpenetration and the stable double nuclear motif of the metal ions. The thermal behavior was confirmed by STA experiments, the mass loss and the detection of the mass signal m/z = 44 (CO_2) via MS-coupling corresponds to decarboxylation of the ligand tdc^{2-}; Figure SI4 of the SI).

The structural motif of $^3_\infty$[Zn(tdc)(bpy)] is depicted exemplarily in Figure 2. Both oxygen atoms of one carboxylic group of each tdc^{2-} bind to a different metal ion (μ_2-η^1:η^1). The second carboxylic group acts as a monodentate or chelating group to only one metal ion depending on the coordinated ion species (μ_1-η^1 or μ_1-η^2). This connectivity leads to a double nuclear motif of the metal ions and to an extended planar 2D network. The M(tdc) planes are additionally connected through the bridging bpy ligands leading to the formation of a 3D network as shown in Figure 2. The same structure motif has already been observed by Jia et al. employing Fe^{2+} and Co^{2+} ions and the same ligands.[22]

Table 1. Crystallographic Data of $^3_\infty$[M(tdc)(bpy)]

$^3_\infty$[M(tdc)(bpy)]	M = Zn^{2+}	M = Co^{2+}	M = Cd^{2+} as synthesized	M = Cd^{2+} after solvent removal
empirical formula	$C_{16}H_{10}N_2O_4SZn$	$C_{16}H_{10}N_2O_4SCo$	$C_{16}H_{10}N_2O_4SCd$	$C_{16}H_{10}N_2O_4SCd$
a [pm]	1138.4(2)	1138.2(2)	1915.88(13)	1170.02(10)
b [pm]	1829.5(3)	1790.7(3)	1169.24(8)	1529.08(18)
c [pm]	1586.8(2)	1617.1(3)	1582.48(9)	1938.46(15)
V [10^6 pm^3]	3304.7(8)	3296.1(10)	3445.0(4)	3468.0(6)
Z	8	8	8	8
crystal system	orthorhombic	orthorhombic	monoclinic[a]	orthorhombic
space group	$P\,ccn$ (No. 56)	$P\,ccn$ (No. 56)	$P\,2/c$ (No. 13)	$C\,mce$ (No. 64)
T [K]	293	213	180	180
$D_{\text{calcd.}}$ [g cm^{-3}]	1.575	1.553	1.644	1.681
$F(000)$	1584	1560	1728	1728
range of data collection [°]	2.23–26.00	2.11–25.80	1.15–27.00	1.15–29.00
reflections collected	13068	16119	11026	5508
independent reflections	3102	3164	7027	1978
observed reflections [$I > 2\sigma(I)$]	1685	1437	6126	1697
number of parameters	217	217	144	127
R_{int}	0.067	0.121	0.074	0.040
R_1 [$I > 2\sigma(I)$]	0.033	0.042	0.140	0.025
wR_2 (all data)	0.063	0.066	0.327	0.055
max./min. electron density	0.3/−0.2	0.6/−0.4	4.1/−5.1	0.4/−0.5

[a] $\beta = 90°$, refined as pseudomerohedral twin.

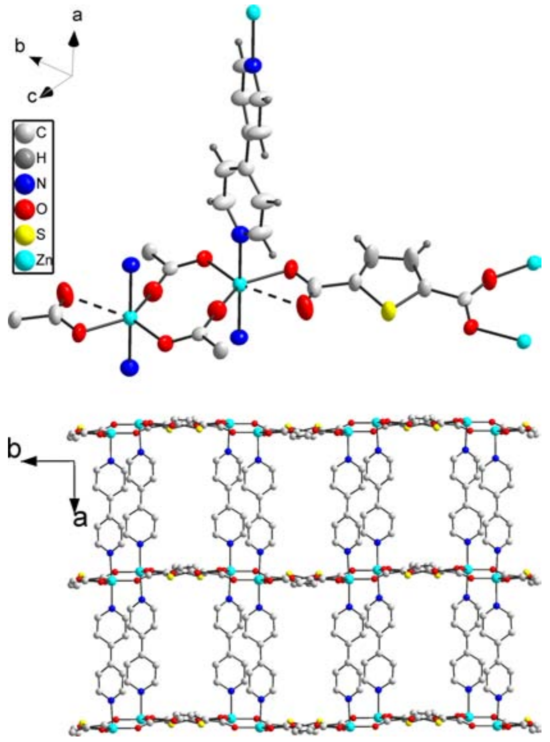

Figure 2. Top: structural motif of $^3_\infty$[M(tdc)(bpy)] for M = Zn^{2+}, tdc^{2-} = 2,5-thiophenedicarboxylate, bpy =4,4′-bipyridine (50% ellipsoids); bottom: overview of a single net of $^3_\infty$[M(tdc)(bpy)] with view along the crystallographic c-axis (H-atoms are omitted for clarity). Zn–donor atom distances are Zn–N 2.140 and 2.156(3); Zn–O 2.004, 2.021, 2.043, and 2.571(2) Å.

The framework of $^3_\infty$[M(tdc)(bpy)] is 2-fold interpenetrated by a second grid. The resulting pore volume calculated by the PLATON routine[23] (9–15% void space depending on the type of metal ions; calculated pore volume in case of Zn^{2+}: 0.077 cm^3/g) was confirmed experimentally by CO_2 adsorption measurements (0.079 cm^3/g calculated by the Gurvich or by the Dubinin–Radushkevich equation; see Figure SI5 of the SI). The phase transition induced by solvent removal can be understood as a movement of the two frameworks (see Figure 3) that results in different atomic positions, different symmetry and therefore in differences in the diffraction pattern (see Figure 1, Figure SI3 of the SI). This can be described crystallographically by an displacive phase transition from the monoclinic space group $P2/c$ (No. 13, $Z = 8$) to the higher symmetric, centered orthorhombic space group $Cmce$ (No. 64, $Z = 8$) with almost the same unit cell dimensions. Whereas the second network in the as synthesized phase ($P2/c$) is generated by inversion from the first one ($-x,-y,-z$), the relationship between the two networks in the solvent free phase is a Bravais translation ($0.5 + x$, $0.5 + y$, z).

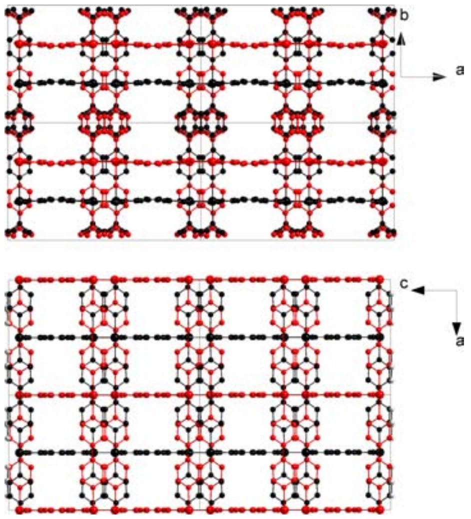

Figure 3. Top: interpenetrated structure of as synthesized $^3_\infty$[Cd(tdc)(bpy)] (space group: $P2/c$); bottom: interpenetrated structure of $^3_\infty$[Cd(tdc)(bpy)] after solvent removal (space group: $Cmce$); the individual nets are colored red and black, respectively.

The comparison of the network structure of $^{3}_{\infty}$[Cd(tdc)(bpy)] with and without solvent molecules (Figure 3) illustrates the changes in the structure induced by solvent removal. While the solvent filled structure has two types of pores (smaller and bigger ones), the solvent free structure with higher symmetry has only one channel size. This can be explained by the loss of interactions of the solvent molecules with the wall of the voids in the network. Thereby, equidistance between the two interpenetrating frameworks without embedded molecules is apparently energetically preferred due to an optimum distance between two layers.

Substitution of $^{3}_{\infty}$[Zn(tdc)(bpy)] by Co^{2+} or Fe^{2+} ions. On the basis of the possibility to create the same structure motif with different metal ions, isomorphous substitution with various amounts of other metal ions was investigated in order to synthesize heteronuclear coordination polymers with catalytically active sites and investigate their catalytic activity. Therefore, substitution of the zinc ions in $^{3}_{\infty}$[Zn(tdc)(bpy)] by various percentages of Co^{2+} or Fe^{2+} ions was performed in order to create heteronuclear coordination polymers. The resulting powder diffraction patterns (see Figure SI 6 of the SI) show the phase purity of the formed mixed metal products and demonstrate the presence of the same structure motif.

As expected, the color changes from white to red or to brown in case of incorporating Co^{2+} and Fe^{2+} ions, respectively (Figure 4). The amount of incorporated foreign ions was analyzed by atomic absorption spectrometry. Applying this substitution method, the resulting incorporation is approximately equivalent to the applied ratio of metal salts as starting materials (Table SI 1 of the SI).

Figure 4. Photograph of the coordination polymers $^{3}_{\infty}[Zn_{1-x}Co_x(tdc)(bpy)]$ in dependence of their Co^{2+} content; from left to right: increasing cobalt content, *x = 0; 0.1; 0.5 and 1.0.*

Catalytic Properties. To evaluate the catalytic properties of the coordination compounds, the oxidation of cyclooctene with *tert*-butyl hydroperoxide as oxidizing agent in liquid toluene was studied. Similar catalytic test reactions were already reported for other MOFs to evaluate the catalytic properties of these materials.[24]

A series of zinc-based coordination polymers with the general formula $^{3}_{\infty}[Zn_{1-x}M_x(tdc)(bpy)]$ substituted by various amounts of Co^{2+} and Fe^{2+} ions, respectively, was examined. The conversion of cyclooctene over the pure zinc compound $^{3}_{\infty}$[Zn(tdc)(bpy)] is identical as in the absence of any catalyst (Figure 5). Interestingly, also the iron(II) substituted coordination compound $^{3}_{\infty}[Zn_{0.9}Fe_{0.1}(tdc)(bpy)]$ is catalytically inactive.

In contrast, the Co^{2+}-based coordination polymer $^{3}_{\infty}$[Co(tdc)(bpy)] is an active catalyst in the oxidation of cyclooctene. Over this catalyst, the cyclooctene conversion reaches 42% after 24 h of reaction (Figure 5) with the epoxide as main product. Note that the conversion over this 3D coordination polymer is much higher than for the Cu-based Basolite C300. For that catalyst, the conversion of cyclooctene reaches only 22% after 24 h. Since the purely Zn-based coordination polymer is inactive, the Co^{2+} sites in the material have to be accessible and active for the catalytic conversion. Although the Co^{2+} ions are 6-fold coordinated in the solid state, one Co−O bond is significantly longer (2.311(3) Å) than the others (1.987−2.109(3) Å). Possibly, dissociation generates a catalytically active site.

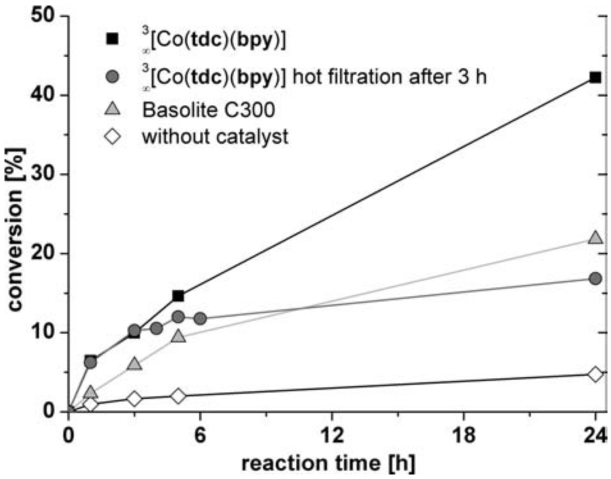

Figure 5. Conversion of cyclooctene over different catalysts and without any catalyst as a function of reaction time.

The heterogeneous nature of the reaction over the Co^{2+}-based coordination polymer $^{3}_{\infty}$[Co(tdc)(bpy)] was proven by a hot-filtration experiment, where the catalyst was removed from the reaction mixture by filtration after 3 h. After catalyst removal, the conversion increases only slightly like in the absence of a catalyst (Figure 5).

It should also be noted that the activity of the materials is directly related to their Co^{2+} content. Thus, samples with an intermediate Co^{2+} content in the series $^{3}_{\infty}[Zn_{1-x}Co_x(tdc)(bpy)]$ also exhibit an intermediate catalytic activity between those of the pure Zn^{2+} and the pure Co^{2+} compound. For instance, the cyclooctene conversion over a sample with $x = 0.25$ amounts to 22% after 24 h. This proves that the catalytic activity depends on the degree of Co^{2+}-substitution while the crystal structure of the catalyst remains unchanged. Details on the catalytic studies including Co^{2+} substitution are reported in an upcoming work.[25]

■ CONCLUSIONS

In summary, four 3D coordination polymers were solvothermally synthesized. Two were previously characterized by Jia et al.[22] All products were extensively characterized by various methods and show phase purity as well as high temperature stability up to approximately 400 °C. A phase transition appearing between 90 and 150 °C was clarified. The calculated (based on structural data) inner surface of $^{3}_{\infty}$[Zn(tdc)(bpy)] was verified by CO_2 adsorption measurements. The Zn^{2+} coordination compound could be modified by incorporation of varying percentages of Fe^{2+} or Co^{2+} ions to create a heteronuclear 3D coordination polymer for applications in catalysis. The amount of substitution was proven by atomic absorption spectrometry. In the catalytic oxidation of cyclooctene with *tert*-butyl hydroperoxide as oxidizing agent and the coordination polymer as catalyst, an increasing conversion of cyclooctene with increasing amount of Co^{2+} ions is observed. Additionally, the conversion of cyclooctene after 24 h over the pure cobalt(II)-containing coordination polymer $^{3}_{\infty}$[Co(tdc)-

(bpy)] as catalyst was significantly higher than in the reaction over Basolite C300 as catalyst (42% vs 22%). In contrast to that, the substitution of Zn^{2+} ions by Fe^{2+} ions did not affect the conversion of cyclooctene. Finally, the heterogeneous character of the reaction was proven by hot filtration experiments. Therefore, it could be shown that the concept of heteronuclear coordination polymers is useful to combine two important requirements: the creation of stable compounds and the tuning of catalytic activity.

■ ASSOCIATED CONTENT

Ⓢ Supporting Information

Crystallographic information files of $^{3}_{\infty}$[M(tdc)(bpy)] (M = Zn^{2+}, Co^{2+}, Cd^{2+}) after solvent removal and additionally of as synthesized $^{3}_{\infty}$[Cd(tdc)(bpy)]; X-ray powder diffraction patterns, STA experiments and gas adsorption isotherms. This material is available free of charge via the Internet at http://pubs.acs.org. CCDC 948050−948053 contain the supplementary crystallographic data for this paper. These data can be obtained free of charge from the Cambridge Crystallographic Data Centre via www.ccdc.cam.ac.uk/data_request/cif.

■ AUTHOR INFORMATION

Corresponding Author

*E-mail: krautscheid@rz.uni-leipzig.de.

Author Contributions

The manuscript was written through contributions of all authors. All authors have given approval to the final version of the manuscript.

Funding

Deutsche Forschungsgemeinschaft (DFG)−SPP 1362: Poröse metallorganische Gerüstverbindungen; International Research Training Group−IRTG: Diffusion in Porous Materials; Universität Leipzig (PbF 1)

Notes

The authors declare no competing financial interest.

■ ACKNOWLEDGMENTS

We gratefully acknowledge Deutsche Forschungsgemeinschaft (DFG−SPP 1362) for financial support. We thank Universität Leipzig (PbF 1) and IRTG "Diffusion in Porous Materials" for supporting this project and Dr. Dirk Friedrich for AAS analyses.

■ REFERENCES

(1) Janiak, C. *Dalton Trans.* **2003**, 2781. Kitagawa, S.; Kitaura, R.; Noro, S. *Angew. Chem., Int. Ed.* **2004**, *43*, 2334. Farrusseng, D., Ed. *Metal-Organic Frameworks: Applications from Catalysis to Gas Storage*; Wiley-VCH, Weinheim, 2011

(2) Lin, R.-B.; Chen, D.; Lin, Y.-Y.; Zhang, J.-P.; Chen, X.-M. *Inorg. Chem.* **2012**, *51*, 9950−9955. Müller, M.; Hermes, S.; Kahler, K.; van den Berg, M. W. E.; Muhler, M.; Fischer, R. A. *Chem. Mater.* **2008**, *20*, 4576−4587. Shultz, A. M.; Farha, O. K.; Hupp, J. T.; Nguyen, S. T. *J. Am. Chem. Soc.* **2009**, *131*, 4204−4205. Li, S.-M.; Zheng, X.-J.; Yuan, D.-Q.; Ablet, A.; Jin, L.-P. *Inorg. Chem.* **2012**, *51*, 1201−1203.

(3) Henninger, S. K.; Habib, H. A.; Janiak, C. *J. Am. Chem. Soc.* **2009**, *131*, 2776. Jeremias, F.; Khutia, A.; Henninger, S. K.; Janiak, C. *J. Mater. Chem.* **2012**, *22*, 10148.

(4) Lässig, D.; Lincke, J.; Moellmer, J.; Reichenbach, C.; Moeller, A.; Gläser, R.; Kalies, G.; Cychosz, K. A.; Thommes, M.; Staudt, R.; Krautscheid, H. *Angew. Chem., Int. Ed.* **2011**, *50*, 10344−10348. Bastos Neto, M.; Patzschke, C.; Lange, M.; Möllmer, J.; Möller, A.; Fichtner, K S.; Schrage, C.; Lässig, D.; Lincke, J.; Staudt, R.; Krautscheid, H.; Gläser, R. *Energy Environ. Sci.* **2012**, *5*, 8294−8303. Moellmer, J.; Moeller, A.; Patzschke, C.; Stein, K.; Lässig, D.; Lincke, J.; Gläser, R.; Krautscheid, H.; Staudt, R. *J. Mater. Chem.* **2012**, *22*, 10274−10286.

(5) Chui, S. S.-Y.; Lo, S. M.-F.; Charmant, J. P. H.; Orpen, A. G.; Williams, I. D. *Science* **1999**, *283*, 1148−1150.

(6) Klein, N.; Senkovska, I.; Gedrich, K.; Stoeck, U.; Henschel, A.; Müller, U.; Kaskel, S. *Angew. Chem., Int. Ed.* **2009**, *48*, 9954−9957.

(7) Aakeröy, C. B.; Champness, N. R.; Janiak, C. *CrystEngComm* **2010**, *12*, 22−43. Habib, H. A.; Sanchiz, J.; Janiak, C. *Inorg. Chim. Acta* **2009**, *362*, 2452−2460. Habib, H. A.; Hoffmann, A.; Höppe, H. A.; Janiak, C. *Dalton Trans.* **2009**, 1742−1751. Habib, H. A.; Sanchiz, J.; Janiak, C. *Dalton Trans.* **2008**, 1734−1744. Wisser, B.; Lu, Y.; Janiak, C. *Z. Anorg. Allg. Chem.* **2007**, *633*, 1189−1192. Henke, S.; Schneemann, A.; Wütscher, A.; Fischer, R. A. *J. Am. Chem. Soc.* **2012**, *134*, 9464−9474.

(8) Guo, H.; Zhu, Y.; Qiu, S.; Lercher, J. A.; Zhang, H. *Adv. Mater.* **2010**, *22*, 4190−4192. Botas, J. A.; Calleja, G.; Sánchez-Sánchez, M.; Orcajo, M. G. *Langmuir* **2010**, *6*, 5300. Botas, J. A.; Calleja, G.; Sánchez-Sánchez, M.; Orcajo, M. G. *Int. J. Hydrogen Energy* **2011**, *36*, 10834.

(9) Pearson, R. G. *J. Am. Chem. Soc.* **1963**, *85*, 3533.

(10) Lysenko, A. B.; Senchyk, G. A.; Lincke, J.; Lässig, D.; Fokin, A. A.; Butova, E. D.; Schreiner, P. R.; Krautscheid, H.; Domasevitch, K. V. *Dalton Trans.* **2010**, 4223−4231. Senchyk, G. A.; Bukhan'ko, V. A.; Lysenko, A. B.; Krautscheid, H.; Rusanov, E. B.; Chernega, A. N.; Domasevitch, K. V. *Inorg. Chem.* **2012**, *51*, 8025−8033.

(11) Fu, Y.; Su, J.; Yang, S.; Zou, Z.; Li, G.; Liao, F.; Xiong, M.; Lin, J. *Cryst. Growth. Des.* **2011**, *11*, 2243−2249. Ahlers, R.; Ruschewitz, U. *Z. Anorg. Allg. Chem.* **2010**, *636*, 11−14.

(12) Mizuno, Y.; Okubo, L M.; Kagesawa, K.; Asakura, D.; Kudo, T.; Zhou, H.; Oh-ishi, K.; Okazawa, A.; Kojima, N. *Inorg. Chem.* **2012**, *51*, 10311−10316. Ferrando-Soria, J.; Serra-Crespo, P.; de Lange, M.; Gascon, J.; Kapteijn, F.; Julve, M.; Cano, J.; Lloret, F.; Pasan, J.; Ruiz-Perez, C.; Journaux, Y.; Pardo, E. *J. Am. Chem. Soc.* **2012**, *134*, 15301−15304.

(13) Zhu, C.; Yuan, G.; Chen, X.; Yang, Z.; Cui, Y. *J. Am. Chem. Soc.* **2012**, *134*, 8058−8061.

(14) An, L.; Zhou, J.; Zhao, L.; Lv, L. *Struct. Chem.* **2010**, *21*, 159−164. Sun, X.-Z.; Sun, Y.-F.; Ye, B.-H.; Chen, X.-M. *Inorg. Chem. Commun.* **2003**, *6*, 1412−1414. Jia, H.-P.; Li, W.; Ju, Z.-F.; Zhang, J. Eur. *J. Inorg. Chem.* **2006**, 4264−4270. Wang, J.-G.; Huang, C.; Huang, X.; Liu, D.-S. *Cryst. Growth Des.* **2008**, *8*, 795−798.

(15) Feringa, B. L.; Hulst, R.; Rikersa, R.; Brandsma, L. *Synthesis* **1988**, *4*, 316−318.

(16) van Pham, C.; Macomber, R. S.; Mark, H. B., Jr.; Zimmer, H. *J. Org. Chem.* **1984**, *49*, 5250−5253.

(17) Sheldrick, G. M. *Acta Crystallogr.* **2008**, *A64*, 112−122.

(18) Farrugia, L. J. *J. Appl. Crystallogr.* **1999**, *32*, 837−838.

(19) Brandenburg, K. *DIAMOND 3.2e*; Crystal Impact GbR: Bonn, 2010.

(20) Moellmer, J.; Möller, A.; Dreisbach, F.; Gläser, R.; Staudt, R. *Microporous Mesoporous Mater.* **2011**, *138*, 140−148.

(21) Lincke, J.; Lässig, D.; Kobalz, M.; Bergmann, J.; Handke, M.; Möllmer, J.; Lange, M.; Roth, C.; Moeller, A.; Staudt, R.; Krautscheid, H. *Inorg. Chem.* **2012**, *51*, 7579−7586.

(22) Jia, H.-P.; Li, W.; Ju, Z.-F.; Zhang, J. *Eur. J. Inorg. Chem.* **2006**, 4264−4270.

(23) Spek, A. L. *J. Appl. Crystallogr.* **2003**, *36*, 7−13.

(24) Leus, K.; Muylaert, I.; Vandichel, M.; Marin, G. B.; Waroquier, M.; Van Speybroeck, V.; Van der Voort, P. *Chem. Commun.* **2010**, *46*, 5085−5087. Tonigold, M.; Lu, Y.; Bredenkötter, B.; Rieger, B.; Bahnmüller, S.; Hitzbleck, J.; Langstein, G.; Volkmer, D. *Angew. Chem., Int. Ed.* **2009**, *48*, 7546−7550. Lu, Y.; Tonigold, M.; Bredenkotter, B.; Volkmer, D.; Hitzbleck, J.; Langstein, G. *Z. Anorg. Allg. Chem.* **2008**, *634*, 2411−2417. Dhakshinamoorthy, A.; Alvaro, M.; Garcia, H. *Catal. Sci. Technol.* **2011**, *1*, 856.

(25) Worch, C.; Kettner, F.; Lässig, D.; Lincke, J.; Krautscheid, H.; Gläser, R. *Catal. Commun.*, *submitted.*